J Therm Anal Calorim
DOI 10.1007/s10973-015-5161-4

Mineralogical and thermal characterization of borate minerals from Rio Grande deposit, Uyuni (Bolivia)

M. Garcia-Valles[1] · P. Alfonso[2] · J. R. H. Arancibia[3] · S. Martínez[1] · D. Parcerisa[2]

Received: 21 July 2015 / Accepted: 12 November 2015

Abstract Large volumes of borate resources exist in Bolivia, with the most important being the Rio Grande deposit, located close to the Salar of Uyuni. Here, borates occur in beds and lenses of variable thickness. A mineralogical and thermal characterization of borates from the Rio Grande was made using XRD, FTIR, SEM and DTA–TG. The deposit is mainly composed of B_2O_3, CaO and Na_2O, with minor contents of MgO and K_2O. Some outcrops are constituted by pure ulexite aggregates ($NaCaB_5O_6(OH)_6{\cdot}5H_2O$) of fibrous morphology; in other cases, gypsum, calcite and halite also are present. The thermal decomposition of ulexite begins at 70 °C and proceeds up to ~550 °C; this decomposition is attributed to dehydration and dehydroxylation processes in three steps: at 115, 150–300 and 300–550 °C. The last weight loss of 1–5 % at 800 °C is due to the removal of Cl_2 from the decomposition of halite. DTA shows two endothermic events related to the removal of water; in the first, $NaCaB_5O_6(OH)_6{\cdot}5H_2O$ evolved from $NaCaB_5O_6(OH)_6{\cdot}3H_2O$, at 108–116 °C; in the second, $NaCaB_5O_6(OH)_6$ is formed at 180–185 °C and $NaCaB_5O_9$ (amorphous) is formed at 300–550 °C. The exothermic peak (658–720 °C) is related to the crystallization of $NaCaB_5O_9$. A small endothermic peak appears due to the halite melting. Later, another endothermic event (821–877 °C) appears, which is related to the decomposition of $NaCaB_5O_9$ into a crystalline phase of CaB_2O_4 and amorphous NaB_3O_5. The XRD pattern evidences that, at 1050 °C, CaB_2O_4 still remains in the crystalline state.

Keywords Borate minerals · Ulexite · Thermal evolution · DTA–TG · XRD · FTIR

Introduction

Bolivia has large volumes of borate resources, the most important being the playa -lake type deposit of the Rio Grande, which has total reserves estimated at approximately 1.6 Mt of boron [1, 2]. This deposit comprises an area of approximately 50 km^2 located close to the southern part of the Salar of Uyuni in the contact between fluvio-deltaic and lacustrine sediments in the Río Grande de Lípez delta. The deposit is being exploited, and borates are commercialized after a natural dehydration process, calcination and grinding.

Borates are classified as critical materials by the European Union [3]. Borate minerals are the main source of boron and have a multitude of industrial applications [4]. In addition to classical applications of boron in glass, ceramics, fertilizers, special alloys, aeronautics, nuclear, military vehicles, fuels, electronics and communications, new uses appear daily, such as for polymeric materials [5] and for imparting halogen-free flame-retardant properties to cellulose-based materials [6]. Ca-, Na-borate minerals are mainly applied for making fiberglass, but are also used for ceramics and ceramic glazes [7, 8]. Other applications reported for Ca-rich borates include nuclear technology [9] and the refractory industry.

✉ M. Garcia-Valles
maitegarciavalles@ub.edu

[1] Dept. Cristallografia, Mineralogia i Dip. Minerals, Fac. Geologia, Universitat de Barcelona, c/ Martí i Franquès, s/n, 08028 Barcelona, Spain

[2] Dept. de Enginyeria Minera i Recursos Naturals, Universitat Politècnica de Catalunya, Avd. de les Bases de Manresa. 61-73, 08242 Manresa, Spain

[3] Dept. de Ingeniería Química, Universidad Técnica de Oruro, C/ 6 de Octubre-Cochabamba, Oruro, Bolivia

Journal : Large 10973 | Dispatch : 17-11-2015 | Pages : 7
Article No. : 5161 | LE | TYPESET
MS Code : JTAC-D-15-00934 | CP | DISK

The industrial uses of borate minerals greatly depend upon its thermal properties. Therefore, to recommend the optimal application of borate minerals, knowing the thermal properties is important.

Numerous studies on the thermal properties of borate minerals have been reported; some of them use mixtures of different borate minerals [10, 11] or a specific mineral, such as ulexite [12–14].

In this paper, we present a mineralogical and thermal characterization of borates from the Rio Grande deposit in Bolivia with special emphasis on the mineralogy of the different events during thermal treatment.

Geological setting

The Bolivian Altiplano is a major basin filled with thick sequences of continental sediments of Cretaceous to Tertiary age [15]. In the quaternary, endorheic basins of the Altiplano were occupied by large lakes, which progressively reduced its size due to intense evaporation and low precipitation that occurred in the region during the last 10,000 years, giving rise to the salt lakes and salars, such as Poopó, Uyuni and Coipasa, in the Central Altiplano.

The western and southern areas of the Altiplano were strongly affected by an intense volcanic activity from the Oligocene to the Quaternary. Volcanic rocks range from andesites to rhyodacites with abundant ignimbrites [2], which are considered to be the source of lithium and boron of the salars and nearby evaporitic deposits [16].

More than 40 borate deposits occur in the Andean belt related to salars [17]. The Rio Grande borate deposit occurs in the southern region of the salar of Uyuni, the largest on Earth, and is composed of deltaic-lacustrine sediments in contact with the salt crust (Fig. 1) [18]. Borates precipitated by capillary rise and subsequent evaporation of the groundwater. Silty sediments occur in contact with the water of the salar; groundwater rises due to porosity and drops evaporate when they reach the surface and the dissolved components precipitate when they come into contact with the water layer. The borate deposit is not in the area of higher concentrations of Li, K and B, but rather further to the south. Ulexite precipitation is controlled by the concentrations of Ca, Na and B in the brine [2].

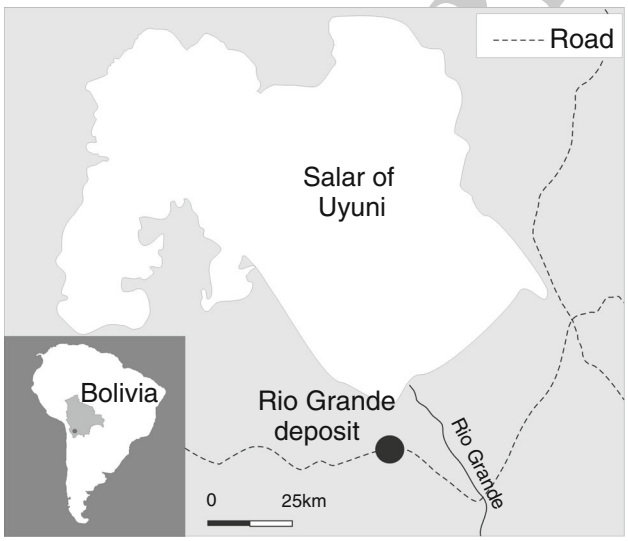

Fig. 1 Location of the Rio Grande borate deposit

In this deposit, borates occur in beds and lenses of variable thickness, from 0.5 to 5 m. In the western region of the deposit, the lenses outcrop in small reliefs of several cm. In the eastern area of the deposit, the bed of borates is present at a depth up to 2 m below the clay level. Borate minerals form brittle nodules with a cotton-ball texture near the surface interbedded within the fluvial-deltaic sediment layers constituted by gypsum, clays and sands. The clays are mainly montmorillonite, illite and kaolinite [2].

Materials and methods

Seven samples of borate minerals were obtained from different outcrops in the Rio Grande deposit along 4.5 km, and all the samples were collected from the natural occurrence in the deposit (Fig. 1).

The chemical composition was determined by inductively coupled plasma mass spectrometry (ICP-MS) using an Agilent 7500ce OPTIMA 3200RL ICP-MS spectrometer with a reaction cell.

The mineralogy of the natural and thermally treated samples was determined by X-ray diffraction (XRD). The AQ2 spectra were obtained from powdered samples (particles under 45 μm) in a Bragg–Brentano PANAnalytical X'Pert Diffractometer system (graphite monochromator, automatic gap, Kα radiation of Cu at $\lambda = 1.54061$ Å, powered at 45 kV, 40 mA, scanning range 4–100° with a 0.017° 2θ step scan and a 50-s measuring time). The identification and semiquantitative evaluation of phases were conducted using a PANanalytical X'Pert HighScore software. Chemical bonds in the borate structure were also characterized by Fourier transform infrared spectroscopy (FTIR). Vibrational spectra were obtained in the 400–4000 cm^{-1} range using a Perkin Elmer Frontier FTIR spectrophotometer. Original borates textures were observed by scanning electron microscopy (SEM) using a Quanta 200 FEI, XTE 325/D8395 environmental scanning electron microscope.

Thermal evolution of each mineral phase and the nature and mechanisms of thermal decomposition were obtained by differential thermal analysis and thermogravimetry

Journal : Large 10973 Dispatch : 17-11-2015 Pages : 7
Article No. : 5161 LE TYPESET
MS Code : JTAC-D-15-00934 CP DISK

(DTA–TG) using a Netzsch equipment (STA 409C model). Analyses were conducted under N_2 inert atmosphere at 80 ml min^{-1} constant flow ratio, using Pt crucible, temperature range 25–1200 °C with a linear rate of temperature gradient set to 10 °C min^{-1}. According to DTA–TG results, to determine the mineral evolution with temperature, the heat treatment temperatures were established with a setting time of half an hour, and subsequent analysis by XRD was performed. The heat treatment ranged from 550 to 1050 °C.

Results and discussion

Chemical composition

The chemical composition of the Rio Grande borate deposit is presented in Table 1. The main components are B_2O_3, between 36.21 and 42.60 wt%, CaO, between 12.70 and 13.74 wt%, and Na_2O, from 7.61 to 13.04 wt%, which suggests that borate minerals constitute the main mineral. In some outcrops, the chemical composition is close to that of pure ulexite ($NaCaB_5{\cdot}5H_2O$) with 42.95 % B_2O_3. In other cases, Na is relatively high. Other elements occur in minor amounts; for example, MgO is up to 1.5 wt%, and K_2O up to 0.67 wt%. Fe, Al, Sr and other elements occur in trace amounts.

Mineralogy

In accordance with the data obtained by the chemical analyses, the XRD patterns show that ulexite ($NaCaB_5O_6(OH)_6{\cdot}5H_2O$) is the main mineral phase in the borate deposit. Among the wide range of over 160 species of borate minerals, ulexite is one of the most economically important [19]. In some cases, it is the only mineral present. However, in most outcrops, other evaporite minerals, mainly halite (NaCl) and gypsum ($CaSO_4{\cdot}2H_2O$), also occur. Figure 2 shows a representative XRD pattern from the Rio Grande deposit.

Ulexite occurs as crystalline aggregates with morphology of elongated fibers oriented parallel to each other along [001], greater than 100 microns in length (Fig. 3a). Equant sodium chloride crystals giving rise to dissolution phantasms are located among ulexite fibers (Fig. 3b). Gypsum also forms euhedral crystals up to several cm in size (Fig. 3c).

Infrared spectroscopy, FTIR (Fig. 4), was used to confirm the mineral phases determined by XRD. Ulexite from Rio Grande shows peaks in different spectral ranges. In general, the first bands correspond to water stretching vibrations and the other bands are simply defined as rhombohedral and tetrahedral borate bending modes. A broad band with several overlapping peaks is displayed between the 3600 and 3150 cm^{-1} region assigned to the stretching vibration mode of the O–H group. The bands at 1667 and 1632 cm^{-1} are assigned to the bending mode of H–O–H and free water, respectively. The asymmetric stretching of three-coordinate boron (BO_3) was observed in the range of 1479–1240 cm^{-1}. The bands between 1240 and 1155 cm^{-1} correspond to B–O–H in plane bending modes. An asymmetric stretching mode of B–O in BO_4 was observed between 1027 and 959 cm^{-1}. The bands at 887–839 and 756 cm^{-1} are assigned to the asymmetric and symmetric stretching of B-O in BO_4, respectively. The band at 663 cm^{-1} is the bending to the symmetric stretching mode of three-coordinate boron. The final peaks, located at 561–546 cm^{-1}, are assigned to the bending modes of BO_4 groups [14].

Thermal evolution

Thermal decomposition of borates is a complex mechanism which involves dehydration, polymorphic transition and

Table 1 Chemical composition of the borates from the Rio Grande deposit

wt%	RG-1a	RG-1b	RG-2	RG-3	RG-4	RG-5	RG-7
CaO	13.38	13.74	11.82	13.83	12.90	13.59	12.70
MgO	0.67	0.42	1.46	0.13	0.69	0.94	1.08
Na_2O	9.71	8.36	13.04	7.61	9.95	9.33	10.90
K_2O	0.22	0.16	0.67	0.02	0.25	0.28	0.41
B_2O_3	41.13	40.99	36.21	42.60	39.34	41.65	38.91
Traces/ppm							
Sr	151	786	230	247	441	140	149
Mn	1.51	16.6	2.23	5.90	8.74	3.17	2.40
Al	16.6	676	10.6	200	87.6	12.1	17.0
Fe	9.39	376	6.75	105	72.7	18.7	18.3
Ti	–	28.1	–	9.52	–	–	–
As	1.90	8.20	2.00	4.30	9.30	3.40	1.60

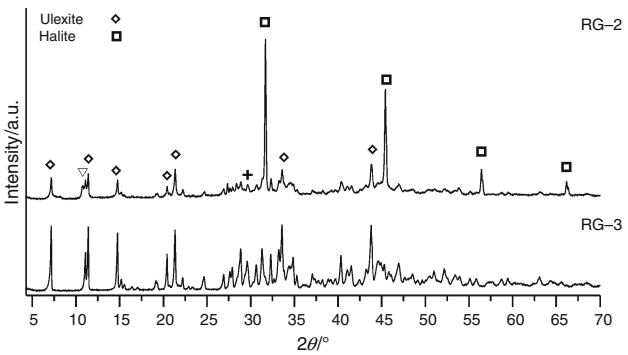

Fig. 2 XRD patterns of two representative samples. RG-2 is the halite rich sample, and RG-3 is nearly pure ulexite

Journal : Large 10973 Dispatch : 17-11-2015 Pages : 7
Article No. : 5161
MS Code : JTAC-D-15-00934
☐ LE ☐ TYPESET
☑ CP ☑ DISK

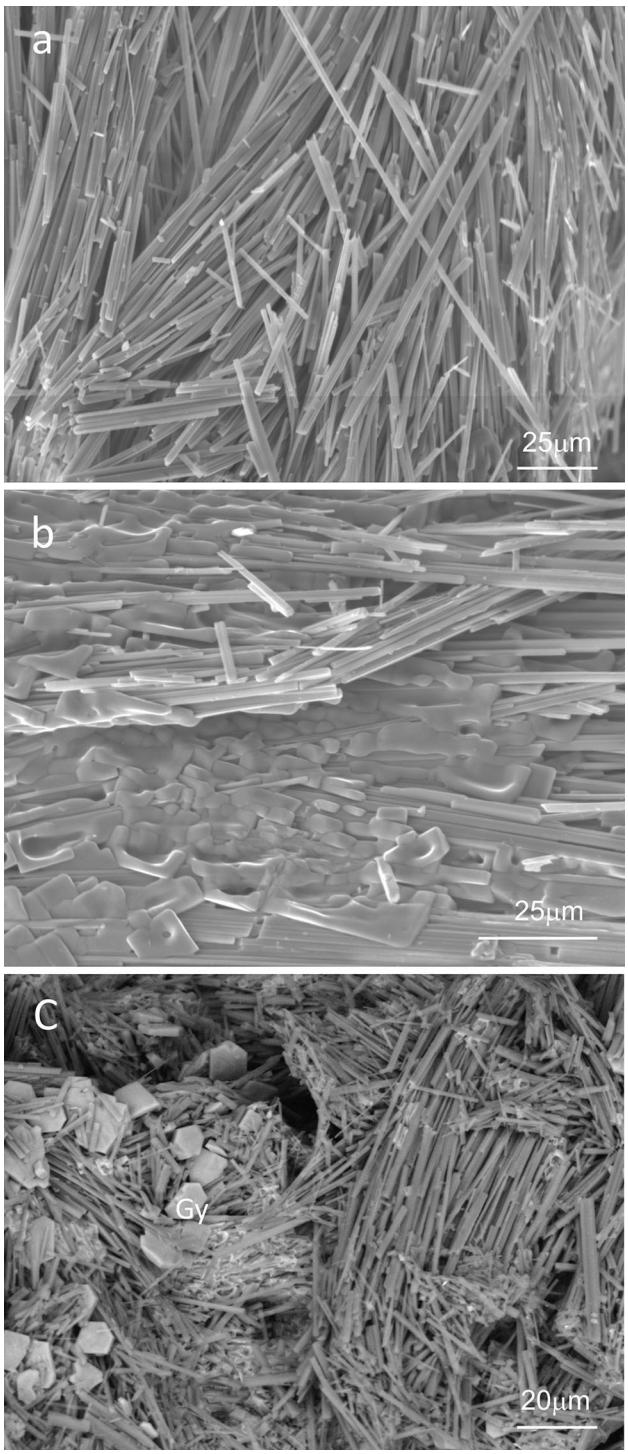

Fig. 3 SEM images of borates from Rio Grande, **a** fibrous ulexite, **b** ulexite with deliquescent halite, **c** ulexite accompanied with euhedral gypsum crystals

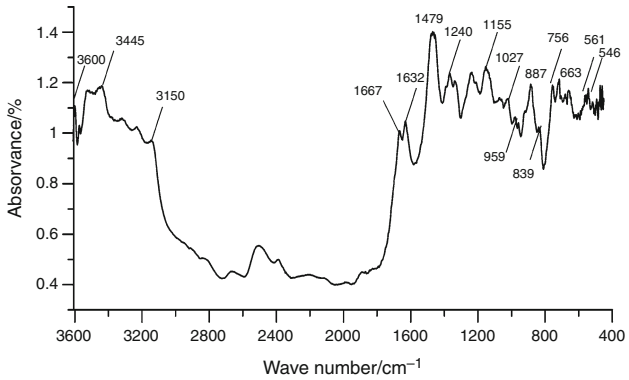

Fig. 4 FTIR spectrum of ulexite from Rio Grande salar

210 solid phase transformation [20]. In the case of ulexite, the
211 decomposition process develops in the different stages
212 shown in the DTA–TG curves (Figs. 5, 6). Decomposition begins at approximately 70 °C and proceeds up to ~550 °C; these temperatures can be attributed to dehydration and dehydroxylation processes [21–23].

The TG curves indicate that these processes present a weight loss in three steps (Table 2); 3.4–5.7 wt% of mass loss is attributed to the release of two molecules of crystal water at approximately 115 °C (1). This loss is lower than the expected for the loss of two molecules of water, which is likely due to sample manipulation. The second loss, 11–14.9 wt%, between 150 and 300 °C, is attributed to the removal of the three molecules of crystal water (2), and the last, 11–16.2 wt% of mass loss is due the release of another three molecules of crystal water, between 300 and 550 °C, that corresponds to dehydroxylation of ulexite (3). Sener et al. [20] indicate that in the first stage of dehydration 1.5 of water molecules is released at approximately 118 °C. During the second stage, between 118 and 260 °C, 0.5 in 2.5 water molecules is lost in two endothermic events. Later, the OH groups are liberated as three water molecules. However, Seyhun et al. [22] attributed the loss of three water molecules to the first event and two molecules to the second event.

Figure 5 shows the TG curve of the pure ulexite sample; in this case, the global weight loss of 33.5 % corresponds to eight water molecules, similar to the results obtained in other studies of ulexite [14, 22].

All samples, with the exception of RG-3, exhibit a final weight loss of 1–5 % at 800 °C due to the removal of chlorine from the decomposition of the sodium chloride present in the samples.

The transformations were controlled by XRD analysis at temperature intervals (Fig. 5). In the DTA analysis, four endothermic and one exothermic events are observed. The first two are related to the removal of the crystal water shown in the TG measurements at the interval of 108–116 °C (1) and 180–185 °C (2) according to the following reactions:

Journal : Large 10973 Dispatch : 17-11-2015 Pages : 7
Article No. : 5161 LE TYPESET
MS Code : JTAC-D-15-00934 CP DISK

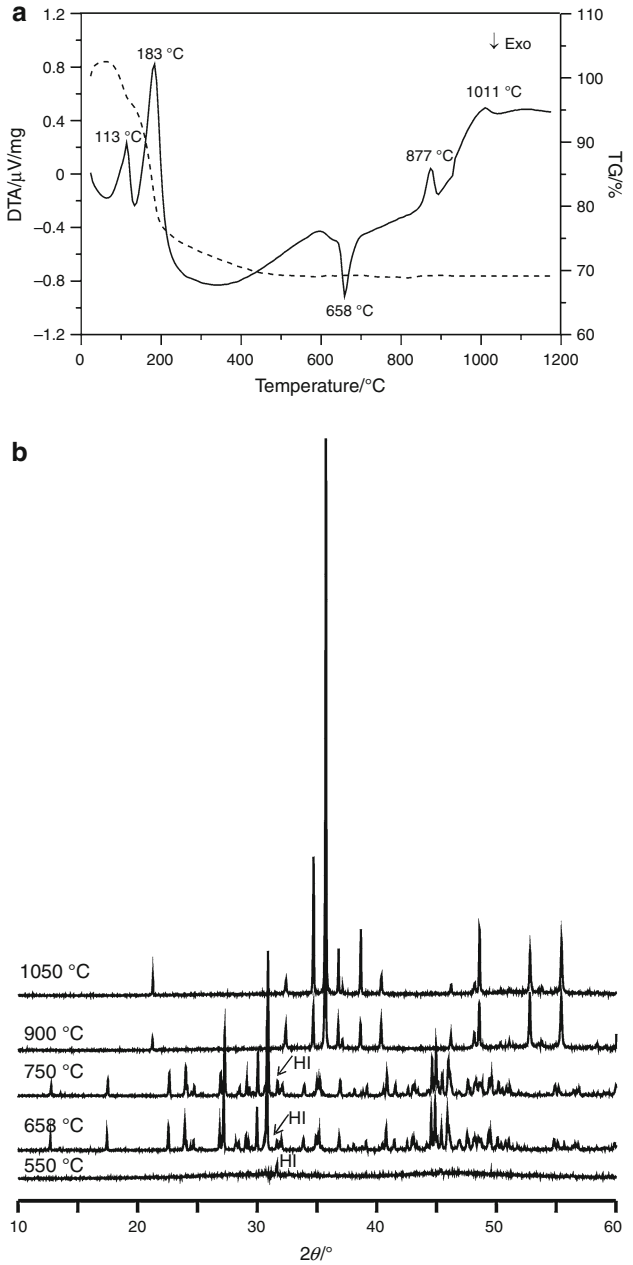

Fig. 5 Pure ulexite (RG-3) **a** DTA–TG curves and **b** sequential XRD patterns showing the new phases formed at each treatment temperature

$$NaCaB_5O_6(OH)_6\cdot 5H_2O \xrightarrow{108-116\,^{\circ}C} NaCaB_5O_6(OH)_6\cdot 3H_2O + 2H_2O \quad (1)$$

$$NaCaB_5O_6(OH)_6\cdot 3H_2O \xrightarrow{180-185\,^{\circ}C} NaCaB_5O_6(OH)_6 + 3H_2O \quad (2)$$

The next reaction, corresponding to the loss of OH groups, did not explicitly show an endothermic phenomenon due to the slow process (3):

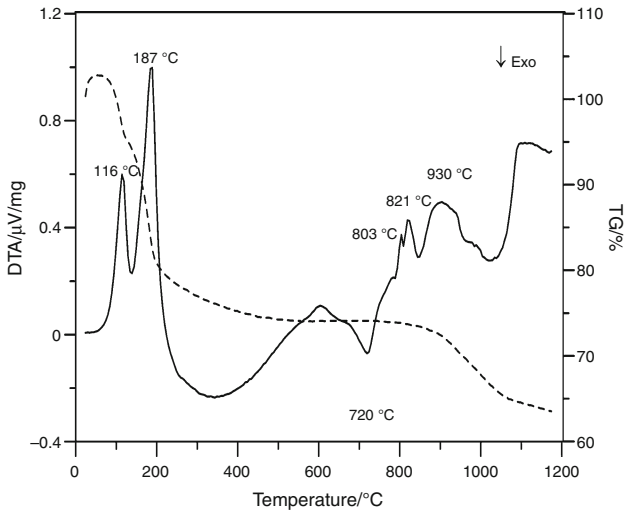

Fig. 6 DTA–TG curves corresponding to a borate sample rich in halite (RG-7)

Table 2 Mass loss (wt%) for different ranges of temperature of the Rio Grande borate deposit

Sample	Range of temperature/°C		
	70–115	150–300	300–550
RG-1a	3.4	12.7	13.6
RG-1b	3.4	14.1	13.4
RG-2	3.4	11.0	11.0
RG-3	4.0	14.4	14.8
RG-4	3.7	12.1	12.8
RG-5	3.6	14.1	14.7
RG-7	5.7	14.9	16.1

$$NaCaB_5O_6(OH)_6 \xrightarrow{300-550\,^{\circ}C} NaCaB_5O_9\ (amorphous) + 3H_2O \quad (3)$$

Ulexite releases eight mol of water in the range of 70–550 °C, and it changes to the $CaNaB_5O_9$ form (amorphous borate phase). The XRD patterns (Fig. 2) show the amorphous structure of the borates at 550 °C. At this temperature, the only crystalline phase present is halite.

The exothermic peak at the interval of 658–720 °C is related to the crystallization process of the amorphous $NaCaB_5O_9$ given as follows (4):

$$NaCaB_5O_9\ (amorphous) \xrightarrow{658-720\,^{\circ}C} NaCaB_5O_9\ (crystalline) \quad (4)$$

When the sample is rich in halite, a new endothermic peak appears near 803 °C due to halite melting (Fig. 6). This temperature increases with the halite content.

The endothermic peak at the interval of 821–877 °C (Fig. 5) is related to the decomposition of $NaCaB_5O_9$ (5).

Journal : Large 10973 | Dispatch : 17-11-2015 | Pages : 7
Article No. : 5161 | LE | TYPESET
MS Code : JTAC-D-15-00934 | CP | DISK

Similar values have been reported for pure ulexite samples [14, 20]. The temperature of this endothermic peak decreases when the halite content increases in the borate sample, up to 821 °C in a sample with 23 wt% of halite (Fig. 6).

$$NaCaB_5O_9\ (\text{crystalline}) \xrightarrow{821-877\,^{\circ}C} CaB_2O_4\ (\text{crystalline}) + NaB_3O_5\ (\text{amorphous}) \quad (5)$$

The thermal evolution of the Rio Grande borates proceeds as mentioned for other ulexite occurrences [20]. On the contrary, other authors, for example Stoch and Waclawska [21], attributed an endothermic peak at 854 °C to the melting temperature of CaB_2O_4. The crystallization of amorphous $NaCaB_5O_9$ directly to CaB_2O_4 and amorphous NaB_3O_5 was also previously suggested.

The melting of the previous phases was reported at 862 °C [14]; Gazualla [24] determined that NaB_3O_5 melted at 873 °C and CaB_2O_4 melted at 1014 °C. Nevertheless, in the present work the experimental temperature reached 1050 °C, and the XRD patterns indicated the presence of crystalline CaB_2O_4 at least up to 1050 °C (Fig. 5). In addition, in the DTA diagram, obtained up to 1200 °C, any endothermic peak characteristic of melting is observed.

The endothermic temperature related to the formation of CaB_2O_4 depends on the alkalis and boron contents. The temperature of $NaCaB_5O_9$ decomposition increases with an increase in the boron ratio in tetrahedral coordination to achieve a maximum value, and then, it decreases again (Fig. 7). This point coincides with the boric anomaly, which occurs at approximately 30 % molar in Na_2O. This reaction is produced without mass loss (Fig. 5).

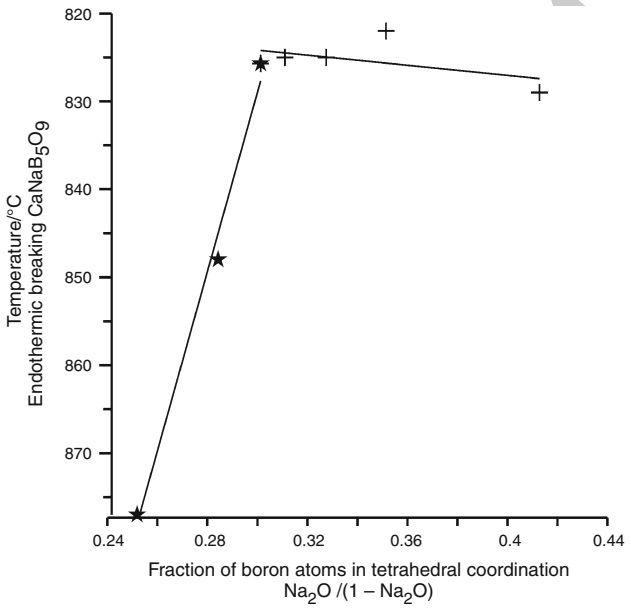

Fig. 7 Representation of the temperature of $NaCaB_5O_9$ decomposition as a function of the fraction of boron atoms in tetrahedral coordination

The crystal structure of $NaCaB_5O_6(OH)_6{\cdot}5H_2O$ has three borate tetrahedra and two borate triangles [25]. When the structure is heated, water is released and $NaCaB_5O_9$ is formed, and the new structure is composed of two borate tetrahedra and three borate triangles [26]. Finally, when the structure decomposes into $CaB_2O_4 + NaB_3O_5$, in the Ca-borate, crystalline, all the boron groups are in a plane triangular coordination [27].

The borate crystal structure was destroyed by dehydration, and an amorphous structure was formed; however, under heat, the crystalline structure is formed again [28]. Then, with the temperature increase, ulexite dehydration causes changes in the stable phases and, thus, in the ratio of tetrahedral and triangular boron coordination.

Conclusions

The Rio Grande borate deposit is mainly comprised of ulexite, as well as occasional other evaporite minerals, such as halite and minor gypsum.

The thermal evolution of ulexite from the studied deposit is shown in the next sequence (6):

$$\begin{aligned} &NaCaB_5O_6(OH)_6{\cdot}5H_2O \\ &\xrightarrow{108-116\,^{\circ}C} NaCaB_5O_6(OH)_6{\cdot}3H_2O + 2H_2O \\ &\xrightarrow{180-185\,^{\circ}C} NaCaB_5O_6(OH)_6 \\ &\xrightarrow{300-550\,^{\circ}C} NaCaB_5O_9\ (\text{amorphous}) + 3H_2O \\ &\xrightarrow{658-720\,^{\circ}C} NaCaB_5O_9\ (\text{crystalline}) \\ &\xrightarrow{821-877\,^{\circ}C} CaB_2O_4\ (\text{crystalline}) + NaB_3O_5\ (\text{amorphous}) \end{aligned} \quad (6)$$

Regarding the heat treatment of borates, this study has shown that, at 1050 °C, the CaB_2O_4 crystalline phase is still present; therefore, the melting temperature will be above this temperature.

The decomposition temperature of $NaCaB_5O_9$ is influenced by the halite content. This temperature decreases when the halite content increases in the sample; however, the halite melting temperature rises with the halite content.

Halite should be removed from borates of the Rio Grande deposit to improve the industrial treatment of borates.

Acknowledgements This research was financed by the Project AECID: A3/042750/11 and the Consolidated Group for Research of Mineral Resources, 2014 SGR-1661) and by the Bosch i Gimpera Fundation Project 307466. The authors would like to thank the staff of the Centres Científics i Tecnològics of the University of Barcelona (CCiTUB) for their technical support.

Journal : Large 10973 | Dispatch : 17-11-2015 | Pages : 7
Article No. : 5161 | LE | TYPESET
MS Code : JTAC-D-15-00934 | CP | DISK

References

1. Risacher F. Origine des concentrations extremes en bore et en lithium dans les saumures de I'Altiplano bolivien. CR Acad Sci Paris Sér. 1984;2(299):701–6.
2. Risacher F, Fritz B. Quaternary geochemical evolution of the salars of Uyuni and Coipasa, Central Altiplano, Bolivia. Chem Geol. 1991;90:211–31.
3. Europen Union. Report on critical raw materials for the EU 2014; pp. 41.
4. Woods WG. An introduction to boron: history, sources, uses, and chemistry. Environ Health Perspect. 1994;102:5–11.
5. Nazari A, Maghsoudpour A, Sanjayan JG. Characteristics of boroaluminosilicate geopolymers. Constr Build Mat. 2014;70: 262–8.
6. Dogan M. Thermal stability and flame retardancy of guanidinium and imidazolium borate finished cotton fabrics. J Therm Anal Calorim. 2014;118:93–8.
7. Stefanov S. Applications of borate compounds for the preparation of ceramic glazes. Glass Technol. 2000;41:193.
8. Christogerou A, Kavas T, Pontikes Y, Koyas S, Tabak Y, Angelopoulos GN. Use of boron wastes in the production of heavy clay ceramics. Ceram Int. 2009;35:447–52.
9. Akan M, Doğan M. Dissolution kinetics of colemanite in oxalic acid solutions. Chem Eng Process. 2004;43:867–72.
10. Waclawwska I. Controlled rate thermal analysis of hydrated borates. J Thermal Anal. 1998;53:519–32.
11. Derun EM, Kipçak AS. Characterization of some boron minerals against neutron shielding and 12 year performance of neutron permeability. J Radioanal Nucl Chem. 2012;291:871–8.
12. Ruoyu C, Jun L, Shuping X, Shiyang G. Thermochemistry of ulexite. Thermochim Acta. 1997;306:1–5.
13. Correcher V, Garcia-Guinea J, Valle-Fuentes FJ. Preliminary study of the thermally stimulated blue luminescence of ulexite. J Therm Anal Calorim. 2006;83:439–44.
14. Piskin MB. Investigation of sodium borohydride production process: "Ulexite mineral as a boron source". Int J Hydrogen Energy. 2009;34:4773–9.
15. Risacher F, Fritz B. Origin of salts and brine evolution of Bolivian and Chilean salars. Aquat Geochem Geol. 2009;15:123–57.
16. Orris GJ. Geology and mineral resources of the Altiplano and Cordillera Occidental, Bolivia: undiscovered nonmetallic deposits. Bull US Geol Surv. 1992;1975:225–9.
17. Helvaci C, Alonso RN. Borate deposits of Turkey and Argentina: a summary and geological comparison. Turkish J Earth Sci. 2000;9:1–27.
18. Marsh SP, Richter DH, Ludington S, Soria-Escalante E, Escobar-Diaz A. Geologic map of the Altiplano and Cordillera Occidental, Bolivia. In: U.S. Geological Survey and Servicio Geologico de Bolivia, Geology and mineral resources of the Altiplano and Cordillera Occidental, Bolivia: U.S. Geological Survey Bulletin; 1975; 365 p. scale 1:500000.
19. Helvaci C, Borates. Encyclopedia Geol. 2005; pp. 510–522. AQ4
20. Şener S, Özbayoğlu G, Demirci Ş. Changes in the structure of ulexite on heating. Thermochim Acta. 2000;362:107–12.
21. Stoch L, Waclawska I. Thermal decomposition of hydrates borates. Thermochim Acta. 1993;215:273–9.
22. Kipcak AS, Derun EM, Piskin S. Characterisation and determination of the neutron transmission properties of sodium–calcium and sodium borates from different regions in Turkey. J Radioanal Nucl Chem. 2014;301:175–88.
23. Erdoğan Y, Zeybek A, Sahin A, Demirbas A. Dehydration kinetics of howlite, ulexite, and tunellite using thermogravimetric data. Thermochim Acta. 1999;326:99–103.
24. Gazulla MF, Gómez MP, Orduña M, Silva G. Caracterización química, mineralogica y térmica de boratos naturales y sintéticos. Bol Soc Ceram Vidr. 2005;44:21–31.
25. Christ CL, Clark JR. A crystal–chemical classification of borate structures with emphasis on hydrated borates. Chem Minerals. 1977;2:59–87.
26. Fayos J, Howie RA, Glasser FP. Structure of calcium sodium pentaborate. Acta Crystallogr C. 1985;41:1394–6.
27. Kirfel A. The electron density distribution in calcium metaborate, $Ca(BO_2)_2$. Acta Crystallogr. 1987;B43:333–43.
28. Tkachenko EA, Fedorov PP, Kuznetsov SV, Voronov VV, Lavrishchev SV, Shukshin VE. Synthesis of nanocrystalline indium orthoborate through borate rearrangement. Russian J Inorg Chem. 2005;50:681–4.

Journal : Large 10973 | Dispatch : 17-11-2015 | Pages : 7
Article No. : 5161 | ☐ LE | ☐ TYPESET
MS Code : JTAC-D-15-00934 | ☑ CP | ☑ DISK

Journal : **10973**
Article : **5161**

Springer
the language of science

Author Query Form

Please ensure you fill out your response to the queries raised below and return this form along with your corrections

Dear Author

During the process of typesetting your article, the following queries have arisen. Please check your typeset proof carefully against the queries listed below and mark the necessary changes either directly on the proof/online grid or in the 'Author's response' area provided below

Query	Details Required	Author's Response
AQ1	Please check the edit made in the sentence 'DTA shows two endothermic events …to the crystallization of NaCaB5O9'.	
AQ2	The term 'PANAnalytical' is used inconsistently with respect to capitalization. Please suggest which occurrence to be followed consistently.	
AQ3	Please check the missing open parenthesis in the sentence 'This research was financed …Gimpera Fundation Project 307466'.	
AQ4	Please update the complete details in Ref. [19].	